# Assessing the Risk and the Uncertainty Affecting the Uncontrolled Re-Entry of Manmade Space Objects

**Carmen Pardini[a1]*, Luciano Anselmo[a2]**

[a] *Space Flight Dynamics Laboratory, Institute of Information Science and Technologies (ISTI), National Research Council (CNR), Via G. Moruzzi 1, 56124 Pisa, Italy*

[1] carmen.pardini@isti.cnr.it; [2] luciano.anselmo@isti.cnr.it

[*] *Corresponding Author*

## Abstract

After a brief review of the risk represented by the uncontrolled re-entry of sizable spacecraft and upper stages, a statistical analysis of 316 predictions issued during the first 20 IADC test campaigns was presented, in order to characterize the errors affecting the estimate of the residual lifetime in the couple of weeks preceding the re-entry. Overall, the mean prediction error was about 10%, increasing to 15% in the last 6 hours. The re-entry predictions for upper stages resulted more accurate than average, with a mean error of about 5%, increasing to approximately 8% during the last day.

In view of the statistical distribution of the predictions, an uncertainty window able to guarantee a confidence level of 90% should generally adopt an amplitude of about ±20% around the estimated nominal re-entry time, to be raised to about ±25% in the couple of days ahead of re-entry. An uncertainty window amplitude of ±30% would be, instead, needed to achieve a confidence level ≥ 95%.

**Keywords:** manmade space objects, uncontrolled re-entry, re-entry predictions, re-entry uncertainty windows, IADC re-entry test campaigns.

## 1. Introduction

Since the beginning of the space age, approximately 24,000 orbiting objects have re-entered into the Earth's atmosphere, accounting for almost 57% of all space objects catalogued by the U.S. Space Surveillance Network (SSN) by the end of 2016. The associated returning mass, both in controlled and uncontrolled re-entries, is now expected to be around 32,000 metric tons, going down to approximately 22,000 metric tons if the re-entries of the Space Shuttle orbiters are taken away [1-3].

Currently, nearly 71% of the decayed objects are represented by orbital debris, while the remaining 29%, totalling most of the mass (~99%), are intact objects, i.e. spacecraft, platforms and spent upper stages. Nowadays, nearly 70% of the re-entries of intact objects are uncontrolled, corresponding to just one half of the returning mass, i.e. about 100 metric tons per year. Over the last decade, there was typically one sizable spacecraft or rocket body uncontrolled re-entry every week, with an average mass approaching 2000 kg.

Through detailed analyses of retrieved spacecraft and rocket body components, it was found that, also in the case of objects not specifically designed to survive the severe mechanical and thermal loads, a mass fraction between 5% and 40% of enough massive bodies might reach the surface of the Earth [4,5].

However, in spite of almost 1900 metric tons of manmade materials, which are suspected to have survived re-entry and hit the ground without control [6], no case of personal injury caused by re-entering artificial debris has been confirmed so far.

The ground casualty risk is still small compared to other commonly accepted risks related to the lifestyle, or the workplace and household safety. For instance, recent evaluations suggest that the risk of being hit by falling orbital debris would be of the order of $10^{-12}$ per human per lifetime, while that of being killed in a car accident would amount to about $10^{-2}$ in industrialized countries [7]. However, it cannot be excluded that uncontrolled re-entries of sizable space objects will became of growing concern in the coming years, due to a combined effect of the increasing use of space and population growth.

Specific guidelines to minimize the risk to human life and property on the ground already exist and are adopted by several organizations around the world. For instance, single re-entries compliant with the NASA standard 8719.14 must have a world-wide human casualty risk not exceeding 0.0001 [8]. In other words, the chance for anybody anywhere in the world of being injured by a piece of falling debris from a single uncontrolled re-entering object must be lower than 1:10,000. Also for the European Space Agency (ESA) the human casualty risk should not exceed 1 in 10,000 for any re-entry event, either controlled or uncontrolled [9,10].

The risk assessment of human casualty from uncontrolled re-entries basically depends on three main factors: 1) The number and casualty area of debris expected to reach the surface of the Earth; 2) The kinetic energy of each surviving fragment; 3) The amount of the world population potentially at risk. A kinetic energy threshold of 15 Joules is typically accepted as the minimum level for potential injury to an unprotected person, while a probability of fatality of 50% corresponds to a kinetic energy of 103 Joules [11]. An important metric to represent and evaluate the potential risk from falling debris is the so-called total debris casualty area [8], which combines in a single figure all information on the breakup process of a re-entering space object. The casualty area of the surviving fragments for a re-entry event is usually computed by means of specific re-entry analysis tools, such as the NASA's Object Re-entry Survival Analysis Tool ORSAT, or the ESA's SpaceCraft Atmospheric Re-entry and Aerothermal Break-up software tool SCARAB [12]. Then, the total human casualty expectation, better known as the casualty expectancy, is obtained as the product of the total debris casualty area and the total average population density in the area overflown by the re-entering object.

Nevertheless, in spite of commonly recognized and worldwide adopted mitigation rules, detailed endo-atmospheric breakup analyses are typically carried out, or disclosed to the public, only for a relatively small number of space objects. In consequence of this, every week or two, on average, an uncontrolled re-entry violating the alert casualty risk threshold of 1:10,000 might probably occur, unknown to most of the governments and safety authorities around the world.

Recognizing the growing concern represented by the uncontrolled re-entry of sizable artificial space objects, the Inter-Agency Space Debris Coordination Committee (IADC) decided to establish a re-entry database for sharing information during IADC re-entry test campaigns, in order to maintain an adequate level of operational readiness to deal with any eventual re-entry emergency. From September 1998 to November 2016, twenty re-entry campaigns have been promoted by the IADC, typically using targets of opportunity, i.e. not necessarily risky space objects. As national technical point of contact, ISTI-CNR has been in charge, for the Italian Space Agency, of all IADC exercises carried out so far.

In spite of decades of efforts, predicting the re-entry time and location of an uncontrolled space object remains an extremely problematic task, being re-entry predictions affected by considerable and unavoidable error sources. For instance, even a few days before the final decay, a typical uncertainty window associated to the re-entry epoch may still include many revolutions, overflying most of the planet,

while in the last few hours the re-entry location may be affected by an along-track uncertainty of more than one full revolution around the Earth.

In this paper, the unavoidable uncertainties affecting re-entry predictions are highlighted and quantified through a detailed analysis of the past IADC re-entry campaigns. Moreover, focusing the attention on a few IADC re-entry events, apparently exceeding the alert casualty risk threshold, the criteria for the activation of a re-entry campaign of national concern are shown. The importance of specific strategies, devised and applied in Italy for civil protection planning and applications, is highlighted as well in such cases.

## 2. IADC re-entry test campaigns

The Inter-Agency Space Debris Coordination Committee is an international governmental forum, established to coordinate worldwide research activities related to space debris (www.iadc-online.org). Among its main objectives there are the exchange of information among the member space agencies, the review of advancements of open actions, and the identification of possible debris mitigation policies.

An IADC action item was open, in 1997, with the intent to establish an informational network for the timely exchange of technical information, e.g. orbit data and re-entry predictions, during re-entry events of potentially hazardous space objects. One year later, in September 1998, the main node of the network, located at the ESA's European Space Operation Centre (ESOC), was tested and approved.

In order to verify the efficiency of the IADC communication network, as well as to enable all participating members to test and improve their prediction tools and procedures, IADC decided to perform regular re-entry campaigns using targets of opportunity, i.e. not necessarily risky space objects (see Fig. 1).

The first IADC exercise was carried out during the second half of October 1998, and a small spacecraft, Inspector, was the test object. Since then, IADC re-entry test campaigns have been generally performed at a mean rate of one per year, with some exceptions related, for instance, to the occurrence of more than one interesting re-entry event in the course of the same year (e.g. the decay of the UARS and ROSAT satellites, in September and October 2011, respectively), or to the worldwide monitoring of the complex final controlled re-entry of the Russian space station Mir, which led to a test campaign gap in 2001. The duration of each campaign was typically 10-15 days, preceding the epoch of the predicted re-entry.

Tab. 1 lists the first twenty IADC re-entry exercises in chronological order, showing the name of the test object with its International Designator, the opening and the closure epoch of the campaign, and the actual reference re-entry epoch at 80 km. In general, the latest was that reconstructed, in a post-event assessment, by the U.S. Strategic Command (USSTRATCOM) and, in almost all cases, it also corresponds to the re-entry epoch of the last Tracking Impact Prediction (TIP) message issued by the USSTRATCOM. From the sixth campaign, i.e. from Cosmos 2332, the final TIP was available with an uncertainty window of ±1 minute in twelve out of fifteen cases.

The largest uncertainties were associated with the post event assessment of the German ROSAT spacecraft (±7 minutes), the Russian satellite Cosmos 1939 (±22 minutes), and the Vega AVUM upper stage (±13 minutes). In the case of Cosmos 1939, due to a considerable delay in the issue of the U.S. post event assessment, and to the quite huge uncertainty (±22 minutes), a reference re-entry time, different from that of the last U.S. TIP, was agreed by the IADC on the basis of the last re-entry estimates uploaded in the IADC re-entry database for this campaign. Therefore, while the last TIP decay epoch was at 15:32 UTC ±22 minutes, on 29 October 2014, the corresponding IADC re-entry time at 80 km was anticipated by 24 minutes, i.e. at 15:08 UTC.

There was also another campaign, involving Cosmos 2332, where the final TIP was incompatible with the observations. In actual fact, while the decay epoch of Cosmos 2332, corresponding to the last TIP, was at 18:05 UTC ±1 minute, on 28 January 2005, both the German FGAN radar and the Russian Space Surveillance System (SSS) were not able to find the re-entering object during expected passes after 16:25 UTC of the same day. Three days afterwards (31 January), a reconstructed re-entry was issued by the U.S. SSN at 16:37 UTC of 28 January 2005. This was assumed as reference re-entry time for Cosmos 2332.

Apart from the decay of the Molniya 3-39 spacecraft, re-entering from a strongly elliptical orbit, all other campaigns considered objects decaying from nearly circular orbits, i.e. with orbital evolution mainly driven by the atmospheric drag perturbation. Seven out of twenty objects were upper stages, while four spacecraft (UARS, ROSAT, GOCE and Phobos-Grunt) were assessed to pose potential risks during re-entry in some countries, including Italy (Fig. 1). For these, re-entry predictions were also carried out for the Italian Space Agency and national civil protection authorities, with the adoption of suitable procedures for risk mitigation purposes.

A peculiar behaviour characterized the re-entry of the ESA's GOCE spacecraft. In fact, after the satellite entered in the Fine Pointing Mode (FPM) phase (with an attitude control minimizing aerodynamic drag during orbital decay), on 21 October 2013, it was expected (according to pre-launch specifications) that this state would have been maintained up to the reaching of an average drag force along the orbit of 20 mN. However, contrary to any expectation, the attitude control system remained operational until re-entry, with drag forces perhaps exceeding 2000 mN [13]. In other words, the GOCE re-entry was "controlled" in some way, and the orbital evolution of this satellite was not compatible with common uncontrolled re-entries. As a consequence, new peculiar and tailored criteria were specifically devised and adopted in this case to assess the re-entry uncertainty windows of use for civil protection applications [13].

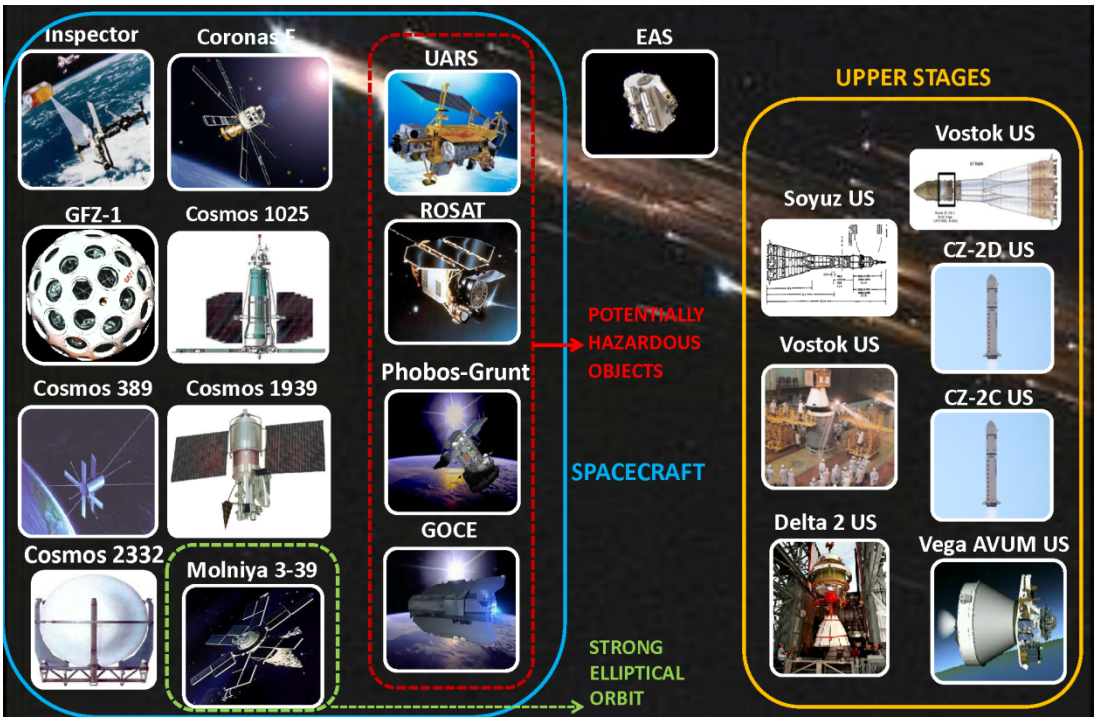


Fig. 1. Test objects (7 upper stages on the right; the Early Ammonia Servicer: EAS in the middle; 12 spacecraft, including 4 objects posing potential risks during re-entry, on the left) used for the first 20 IADC re-entry campaigns

Table 1. List of the first 20 IADC re-entry test campaigns.

| No. | Satellite name | Epoch of the Campaign (Start/End) | Assessed re-entry epoch at 80 km |
|---|---|---|---|
| **1** | **Inspector** 1997-058D | 15 Oct. 1998 16 Nov. 1998 | 1 Nov. 1998 19:49 UTC |
| **2** | **GFZ-1** 1986-017JE | 31 May 1999 24 June 1999 | 23 June 1999 01:21 UTC |
| **3** | **Soyuz US** 1999-058E | 7 Feb. 2000 7 Mar. 2000 | 4 Mar. 2000 05:50 UTC |
| **4** | **Vostok US** 1978-094B | 9 Jan. 2002 21 Jan. 2002 | 19 Jan. 2002 22:09 UTC |
| **5** | **Cosmos 389** 1970-113A | 10 Nov. 2003 25 Nov. 2003 | 24 Nov. 2003 22:36 UTC |
| **6** | **Cosmos 2332** 1996-025A | 17 Jan. 2005 28 Jan. 2005 | 28 Jan. 2005 16:37 UTC |
| **7** | **Coronas F** 2001-032A | 29 Nov. 2005 6 Dec. 2005 | 6 Dec. 2005 17:24 UTC |
| **8** | **Cosmos 1025** 1978-067A | 2 Mar. 2007 10 Mar. 2007 | 10 Mar. 2007 12:56 UTC |
| **9** | **Delta 2 R/B** 2007-023B | 6 Aug. 2007 16 Aug. 2007 | 16 Aug. 2007 09:23 UTC |
| **10** | **EAS** 1998-067BA | 22 Oct. 2008 3 Nov. 2008 | 3 Nov. 2008 04:51 UTC |
| **11** | **Molniya 3-39** 1990-084A | 19 June 2009 9 July 2009 | 8 July 2009 22:42 UTC |
| **12** | **Vostok US** 1979-093B | 20 Apr. 2010 30 Apr. 2010 | 30 Apr. 2010 16:44 UTC |
| **13** | **UARS** 1991-063B | 13 Sept. 2011 24 Sept. 2011 | 24 Sept. 2011 04:00 UTC |
| **14** | **ROSAT** 1990-049A | 10 Oct. 2011 23 Oct. 2011 | 23 Oct. 2011 01:50 UTC |
| **15** | **Phobos-Grunt** 2011-065A | 2 Jan. 2012 15 Jan. 2012 | 15 Jan. 2012 17:46 UTC |
| **16** | **GOCE** 2009-013A | 21 Oct. 2013 12 Nov. 2013 | 11 Nov. 2013 00:16 UTC |
| **17** | **Cosmos 1939** 1988-032A | 15 Oct. 2014 29 Oct. 2014 | 29 Oct. 2014 15:08 UTC |
| **18** | **CZ-2D** 2014-051C | 1 June 2015 14 June 2015 | 14 June 2015 23:58 UTC |
| **19** | **CZ-2C** 2012-064D | 15 June 2016 28 June 2016 | 27 June 2016 19:04 UTC |
| **20** | **AVUM** 2012-006K | 18 Oct. 2016 2 Nov. 2016 | 2 Nov. 2016 04:43 UTC |

The masses of the IADC test objects ranged from a minimum of 20 kg, for the GFZ-1 satellite (followed by the satellite Inspector with 68.5 kg), to a maximum of 13,500 kg, including propellants, for the Phobos-Grunt probe (its dry mass was instead 2350 kg). The heaviest spacecraft was the NASA's Upper Atmosphere Research Satellite (UARS), with a dry mass of 5668 kg, followed by two Chinese Long March upper stages, weighting about four metric tons each. A distribution of the masses is shown in Fig. 2, where for Phobos-Grunt the dry mass is represented, instead of the wet one, including propellants.

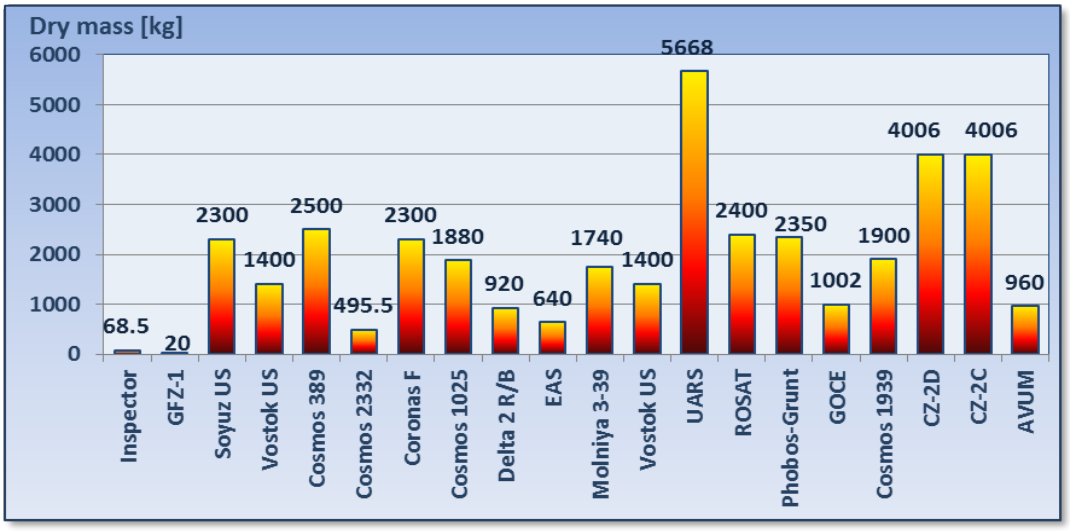


Fig. 2. Dry mass for each IADC re-entry campaign test object

## 3. Solar and geomagnetic activity during the IADC test campaigns

The first 20 IADC re-entry campaigns were distributed over a time span including more than one and half solar activity cycle of about 11 years, as shown in Fig. 3, where the evolution of solar activity is represented, from January 1998 to January 2017, in terms of the daily observed and 81-day averaged solar radio flux at 10.7 cm ($F_{10.7}$), expressed in solar flux units (1 sfu = $10^{-22}$ $Wm^{-2}Hz^{-1}$). The solar activity index $F_{10.7}$, which since the 1960s has been found to be fairly well correlated with the solar extreme ultraviolet (EUV) radiation (i.e. the main responsible of density variations in the thermosphere), is the proxy of this radiation in the atmospheric density models used during the IADC campaigns, namely JR-71 [14], MSIS-86 [15], MSISE-90 [16], NRLMSISE-00 [17], GOST-2004 [18], JB2006 [19].

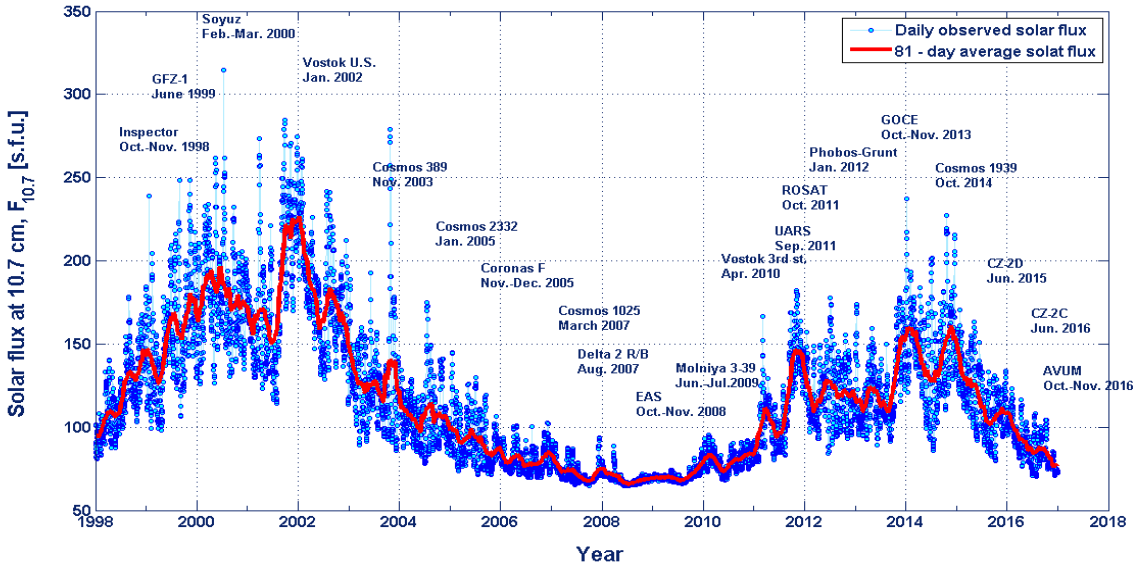


Figure 3. Evolution of solar activity, in terms of the daily observed and 81-day averaged solar flux at 10.7 cm ($F_{10.7}$)

From Fig. 3, it is evident that the campaign of the Vostok upper stage (1978-094B), in January 2002, occurred during the maximum peak of solar cycle 23 (May 1996 – January 2008), while the decay of the Early Ammonia Servicer (EAS), jettisoned from the International Space Station on 23 July 2007 and re-entered in November 2008, was at the minimum of the current solar cycle 24 (start date: January 2008). However, due to the relatively short duration of each campaign, i.e. nearly 10-15 days, and to a rather low number of test cases across specific environmental conditions, it was not possible to systematically investigate the correlation between solar activity levels and the accuracy of re-entry predictions.

Concerning the geomagnetic activity, a few geomagnetic storms, ranging from a minor (geomagnetic planetary index $K_P \sim 5$) to a strong level ($K_P \sim 7$) (www.swpc.noaa.gov/noaa-scales-explanation), occurred during some IADC campaigns. They are represented in Fig. 4, in terms of the maximum values of the planetary geomagnetic indices $K_P$ and $A_P$ recorded during the re-entry campaigns.

However, for all the test objects shown in Fig. 4, no significant geomagnetic storm was registered during the last 48 hours of orbital decay. Overall, the largest storm ($K_P = 7.2$) occurred on 20 November 2003, around 4 days before the re-entry of Cosmos 389.

It cannot be excluded that such storms had played an appreciable role in anticipating the decay time of the re-entering objects affected by them, but being combined with other effects, it was not possible to distinctly extrapolate their effective contribution.

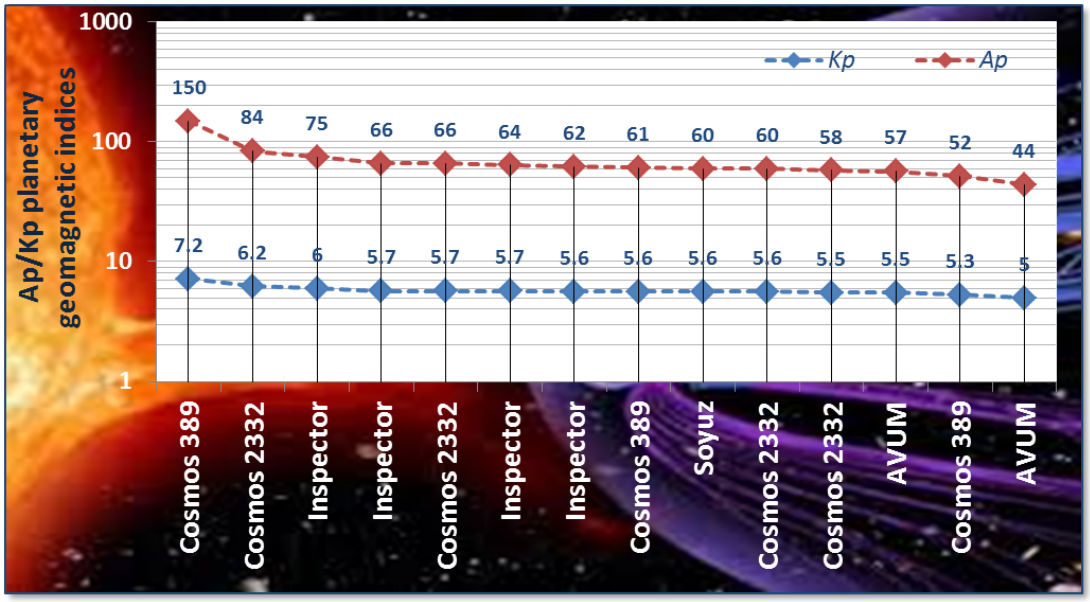


Figure 4. Geomagnetic storms recorded during the IADC re-entry campaigns

## 4. Software tools and atmospheric density models

The ISTI-CNR Satellite Re-entry Analysis Program (SATRAP), originally developed for re-entry predictions [20], but actually applicable to all the circumterrestrial orbital regimes [21], was used to propagate the trajectory in all IADC campaigns. All the principal orbital perturbations were considered, i.e. the geopotential zonal and tesseral harmonics up to the 16$^{th}$ degree and order, the third body attraction of the Sun and the Moon, the direct solar radiation pressure with eclipses, and the aerodynamic drag.

Another ISTI-CNR software tool, named CDFIT, sharing the same force models, physical constants and propagation options of SATRAP, was used to compute the satellite ballistic parameter ($B$), defined as:

$$B = \frac{A \times C_D}{M} \tag{1}$$

where $C_D$, $A$ and $M$ are, respectively, the satellite drag coefficient, the average cross-sectional area and the mass. Having fixed the area-to-mass ratio $A/M$, CDFIT was used to solve for the drag coefficient able to minimize the root mean square residuals ($R$) between the propagated and the observed semi-major axis, the latter inferred from the orbit data, e.g. the Two-Line Elements (TLE) sets, available in the time span of interest:

$$R = \sqrt{\frac{\sum_{i=1}^{N} \left[ a_{i\_obs} - a_{i\_com} \right]^2}{N}} \tag{2}$$

where $a_{i\_obs}$ and $a_{i\_com}$ are, respectively, the observed and the computed semi-major axis at the same epoch and $N$ is the number of observations available, i.e. the number of TLEs used. In such a way, the satellite ballistic parameter, or the drag coefficient if the area-to-mass ratio was maintained constant, was adjusted to force the atmospheric density model to agree with the air drag revealed by the tracking data, i.e. the historical TLE record in the time span of interest.

For each object, the ballistic parameter so obtained, through a retro-fit of the observed semi-major axis decay up to the epoch of the current re-entry prediction, was used by SATRAP to propagate the last TLE available. The satellite ballistic parameter was then recomputed for each prediction carried out, and its fitted value was such to absorb possible biases affecting the air density computation, as well as changes of the satellite cross-sectional area, or attitude (if there is not a loss of components, or propellants, during the orbital decay, the satellite mass typically does not change), up to the current time of the propagation.

Various atmospheric density models were implemented over the years both in SATRAP and in CDFIT. In the current versions they are the following: JR-71 [14], MSIS-86 [15], MSISE-90 [16], NRLMSISE-00 [17], GOST-2004 [18], JB2006 [19] and JB2008 [22]. In almost all campaigns, re-entry predictions were obtained by using and comparing, at the same time, different thermospheric density models selected among those implemented.

However, because one prediction at a time had to be uploaded in the IADC re-entry database, only the models used for the IADC predictions are displayed hereinafter. In seventeen out of twenty campaigns, all the predictions issued to IADC were obtained using one air density model per campaign. In the remaining three exercises, different predictions were instead computed with different density models.

In the seventeen cases in which all the predictions issued to IADC were obtained with a single model, the following models were used: JR-71 during the re-entry campaigns of Inspector, GFZ-1, Cosmos 398, Cosmos 2332, and of the Soyuz and Delta 2 upper stages; MSIS-86 for the Vostok upper stage re-entered in 2002; MSISE-90 for Coronas F and Cosmos 1025; GOST-2004 for Molniya, UARS, ROSAT, Phobos-Grunt and the Vostok upper stage re-entered in 2010; NRLMSISE-00 for GOCE, CZ-2D and AVUM. Instead, during the campaigns of the remaining three test objects, i.e. EAS, Cosmos 1939 and CZ-2C, re-entry predictions obtained with different density models were issued to IADC. NRLMSISE-00, JR-71 and JB2006 were used for EAS, while both NRLMSISE-00 and GOST-2004 were employed for Cosmos 1939 and CZ-2C.

## 5. Re-entry prediction process and uncertainty windows

Once the object's ballistic parameter is determined with CDFIT, using a specific air density model and considering all the relevant orbital perturbations, the last available state vector of the object is (generally) propagated with SATRAP assuming the same orbital perturbations, density model and value of *B*. The trajectory may be propagated up to the reaching of a user defined geodetic re-entry altitude, down to ground impact. But of course, in the case of uncontrolled re-entries, the objects usually break apart just below 80 km, so a propagation down to that altitude makes more sense, dealing with objects still nearly intact. However, if, as for the IADC test campaigns, a different "conventional" reference altitude is adopted, e.g. 10 km, assuming a "fictitious" object remaining intact throughout the endo-atmospheric phase, a hypothetical re-entry down to such reference geodetic height can be estimated as well. The time of flight, between 80 and 10 km, of the re-entering objects assumed to remain intact is anyway quite short, of the order of 7 minutes.

For re-entry events from nearly circular orbits, mainly driven by the atmospheric drag perturbation, the estimate of the re-entry epoch is affected by considerable uncertainties. These can be due to sometimes sparse and inaccurate tracking data, to a complex shape and unknown attitude evolution of the re-entering object, to biases and stochastics inaccuracies affecting the computation of the atmospheric density, to prediction errors of the solar and geomagnetic activity, as well as to the mismodelling of the object's drag coefficient. As a consequence, even if the "best" models and procedures are applied, it is not possible to eliminate some unavoidable error sources. Therefore, the main objective of a re-entry prediction process is to determine the time interval (or re-entry uncertainty window) in which the natural re-entry of a satellite can be foreseen, within a given confidence level, taking into account all the possible uncertainties affecting re-entry predictions.

The definition of appropriate re-entry uncertainty windows is obviously a very critical aspect of the prediction process and is typically based on past lessons and knowledge. The experience accumulated worldwide shows that a relative prediction error of ±20% might be often adopted, in order to reasonably cover all possible error sources. However, in some specific cases, more conservative prediction errors, up to ±30% or more, should be considered, in particular during the last 2-3 days of residual lifetime.

Overall, similar criteria were adopted to define the re-entry uncertainty windows for the IADC campaigns. In fourteen out of twenty cases, it was assumed a percentage variation of the "fitted" ballistic parameter, hopefully able to include errors in the solar and geomagnetic activity forecasts, in the air density estimate, as well as possible changes of the satellite attitude and drag coefficient. This was $B$±20% (start of the re-entry uncertainty window: $B$+20%; end of the window: $B$–20%) for the campaigns 1-4 (Inspector, GFZ-1, Soyuz upper stage, Vostok upper stage re-entered in 2002), 6-10 (Cosmos 2332, Coronas F, Cosmos 1025, Delta 2 rocket body, EAS), and 12-14 (Vostok upper stage re-entered in 2010, UARS, ROSAT). A larger variation of $B$ ($B$±25%) was instead assumed for the campaigns 5 (Cosmos 389) and 17 (Cosmos 1939). In the first case because, during the previous campaign involving the Vostok upper stage decayed in 2002 at a peak of solar activity, a re-entry window obtained by varying $B$ by ±20% had not been able to include all the error sources. In the second case, a variation of $B$ by ±25% was chosen in the attempt to maintain a conservative definition of the window, without the need to change it during the last 2 days before re-entry.

Adopting a given percentage variation of the ballistic parameter leads, of course, to a re-entry window asymmetric with respect to the nominal predicted re-entry time, with the window "head" (before nominal re-entry) shorter than the window "tail" (after nominal re-entry). However, this makes physical sense and the prediction statistics presented afterwards in this paper support the adoption of such asymmetric uncertainty windows.

For 5 campaigns (11, 15, 18, 19, 20, namely Molniya 3-39, Phobos-Grunt, CZ-2D, CZ-2C and AVUM, respectively) the re-entry uncertainty window was instead computed by assuming a percentage variation of the object's residual lifetime. For the re-entry from the highly elliptical orbit of the Molniya 3-39 spacecraft, the residual lifetime was varied by ±30%, and ±20% during the last predictions. During the Phobos-Grunt campaign, the chosen uncertainty window of ±25% of the residual lifetime was found adequate to include the error sources affecting the orbital decay.

For the last three IADC campaigns, i.e. 18-20, a new simplified rule was devised with the intent to define re-entry uncertainty windows with a general confidence level of 90%, based on statistical analysis of past re-entry predictions [23]. It was therefore assumed an error on the residual lifetime of ±20% up to 12 days preceding the predicted decay, then the uncertainty window was linearly increased, during the following 10 days, up to a variation of the residual lifetime of ±30%, effective and maintained fixed during the last two days.

Concerning GOCE (i.e. the 16$^{th}$ campaign), the criteria adopted were completely different and not comparable with uncontrolled re-entries, because a stable attitude was maintained, but with a large uncertainty affecting the operational limits of the actuators [13].

Figs. 5, 6 and 7 show the evolution of the re-entry uncertainty windows for the twenty IADC campaigns, as a function of the residual lifetime. Fig. 5 encompasses all the campaigns duration, Fig. 6 reflects the situation in the last two days, while Fig. 7 refers to the last day.

Considering all the IADC campaigns, a total of 316 re-entry predictions were issued. Tab. 2 lists, for each one, the number of predictions issued overall, during the last two days, and during the last day before re-entry. If the re-entry predictions for the Molniya satellite (decaying from a highly elliptical orbit and then atypical with respect to the other uncontrolled re-entries from nearly circular orbits) and for the GOCE spacecraft (its orbital decay was quite uncommon, as its attitude was controlled until re-entry) are excluded from the tally, a total of 275 predictions was issued.

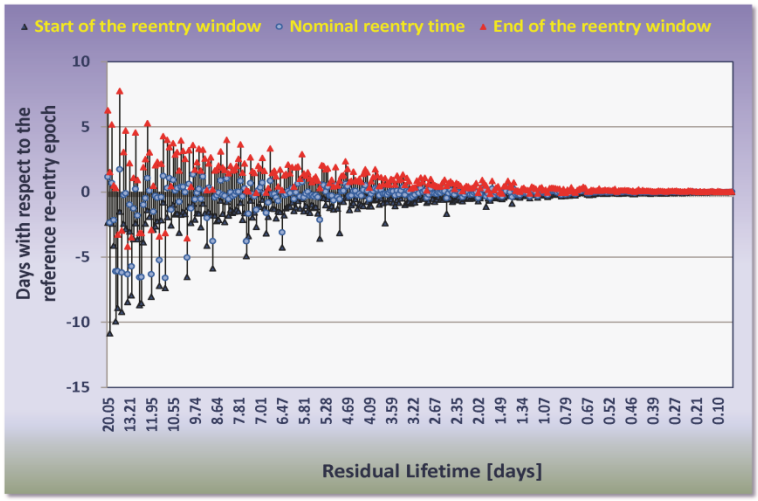


Figure 5. Re-entry uncertainty windows for all the IADC re-entry campaigns

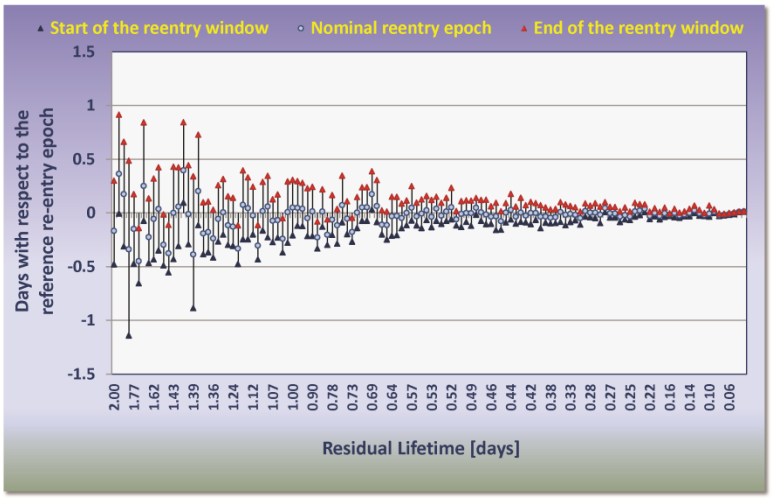


Figure 6. Re-entry uncertainty windows for all the IADC re-entry campaigns during the last two days

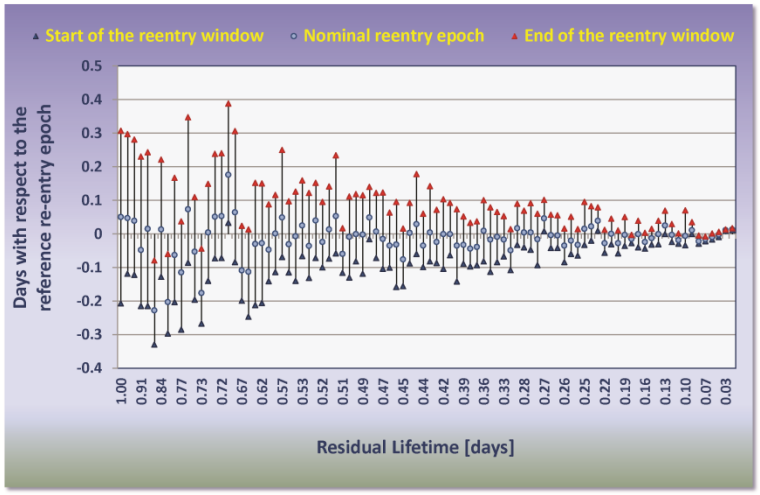


Figure 7. Re-entry uncertainty windows for all the IADC re-entry campaigns during the last day

Through an attentive analysis of the results shown in Figs. 5-7, it was possible to identify the number of uncertainty re-entry windows not including the actual reference re-entry epoch, i.e. those computed assuming prediction errors lower than the actual ones. Overall, 29 out of 316 uncertainty windows (i.e. ~9%) did not include the reference re-entry time. They were 17 out of 127 (i.e. ~13%) during the last two days, 11 out of 91 (i.e. ~12%) during the last day, and 7 out of 57 (i.e. ~12%) during the last 12 hours.

Excluding the predictions issued for the Molniya and GOCE satellites, the re-entry windows for which the error sources were underestimated reduced to 19 out of 275 (i.e. ~7%) over all the campaigns. During the last two days, their numbers remained unchanged, but the percentages of uncertainty window violation became ~15% during the last 2 days, ~14% during the last day, and ~14% during the last 12 hours.

Table 2. Number of re-entry predictions issued during the IADC campaigns.

| Satellite name | Predictions issued during the campaign | Predictions issued during the last two days | Predictions issued during the last day |
|---|---|---|---|
| Inspector | 12 | 1 | 1 |
| GFZ-1 | 8 | 5 | 3 |
| Soyuz US | 15 | 4 | 3 |
| Vostok US | 12 | 6 | 5 |
| Cosmos 389 | 20 | 9 | 8 |
| Cosmos 2332 | 20 | 10 | 7 |
| Coronas F | 13 | 8 | 5 |
| Cosmos 1025 | 19 | 7 | 4 |
| Delta 2 RB | 5 | 1 | 1 |
| EAS | 24 | 10 | 8 |
| Molniya | 19 | 5 | 4 |
| Vostok US | 22 | 9 | 5 |
| UARS | 25 | 13 | 8 |
| ROSAT | 19 | 6 | 6 |
| Phobos-Grunt | 21 | 9 | 6 |
| GOCE | 22 | 8 | 6 |
| Cosmos 1939 | 8 | 5 | 4 |
| CZ-2D | 11 | 4 | 2 |
| CZ-2C | 13 | 5 | 4 |
| AVUM | 8 | 2 | 1 |
| Total | **316** | **127** | **91** |

## 6. Errors in the estimation of the residual lifetime

For each IADC campaign and re-entry prediction, the percentage error affecting the estimate of the residual lifetime ($PE_{RL}$) was computed as follows:

$$PE_{RL} = 100 \times \frac{T_{PRED} - T_{REF}}{T_{REF} - T_{IN}} \tag{3}$$

where $T_{PRED}$ was the predicted re-entry time, $T_{REF}$ the actual reference re-entry epoch, as in Tab. 1, and $T_{IN}$ was the initial epoch of the propagated state vector, which was generally the last available orbit determination of the re-entering object. A mean prediction (*MPE*) error was also determined for each campaign as follows:

$$MPE = \sum_{n=1}^{N_P} \frac{|PE_{RL}|}{N_P} \tag{4}$$

being $N_P$ the number of predictions issued between the current residual lifetime ($RL = T_{REF} - T_{IN}$) and the reference re-entry epoch ($T_{REF}$).

Fig. 8 shows, for each campaign, the number of times the residual lifetime was overestimated, i.e. $PE_{RL} > 0$ and $T_{PRED} > T_{REF}$ (in blue), or underestimated, i.e. $PE_{RL} < 0$ and $T_{PRED} < T_{REF}$ (in red). Considering all the IADC campaigns, it was found that the residual lifetime was overestimated in 123 out of 316 issued predictions, i.e. in about 39% of the cases, and underestimated in 194 predictions, i.e. in nearly 61% of the cases. This asymmetry was slightly reduced if the GOCE and Molniya campaigns were excluded, but remained significant. In fact, among the 275 issued predictions, the residual lifetime was overestimated in 119 cases (~43%) and underestimated in 157 cases (~57%). These results seem to support the adoption of asymmetric re-entry uncertainty windows, with "tails" longer than "heads", as those resulting by varying of a given percentage the ballistic parameter *B* with respect to the nominal value.

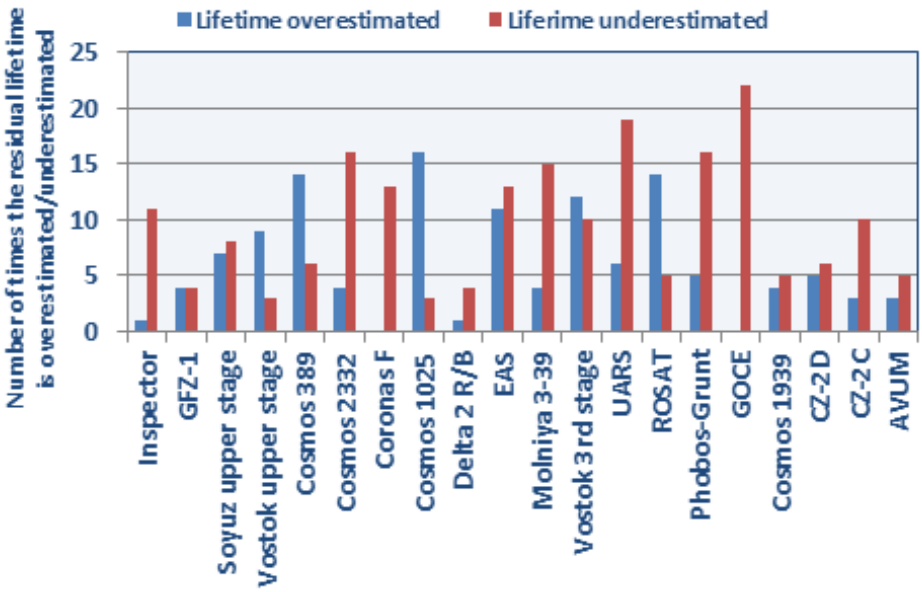


Figure 8. Distribution of the number of times the residual lifetime was overestimated (in blue) or underestimated (in red) during the IADC re-entry campaigns, totalling 316 issued re-entry predictions

Considering all the 316 re-entry predictions issued during the IADC campaigns, the absolute percentage error, $|PE_{RL}|$, affecting each estimate of the residual lifetime is represented in Fig. 9. Overall, the average error was 9.7%. However, the huge errors obtained between 20 and 5 days before re-entry were associated with the GOCE and Molniya re-entry campaigns, which cannot be compared with the usual cases involving uncontrolled orbital decays driven by air drag, as previously explained. Without the predictions for GOCE and Molniya, the remaining 275 forecasts had the absolute percentage errors shown in Fig. 10. Here, the average error affecting each estimate of the residual lifetime was 7.4%.

In Fig. 10 there are still two large relative errors (> 30%) at less than 2 hours ahead of re-entry. These were associated with the Vostok upper stage re-entered in 2002 (44% at 36 minutes before re-entry), and with GFZ-1 (79% at 24 minutes before re-entry). However, it must be remarked that these large relative errors were obtained with probably uncertain state vectors, with epochs very close to the final decay, when only a few minutes of error translate in quite huge percentage uncertainties on the residual lifetime.

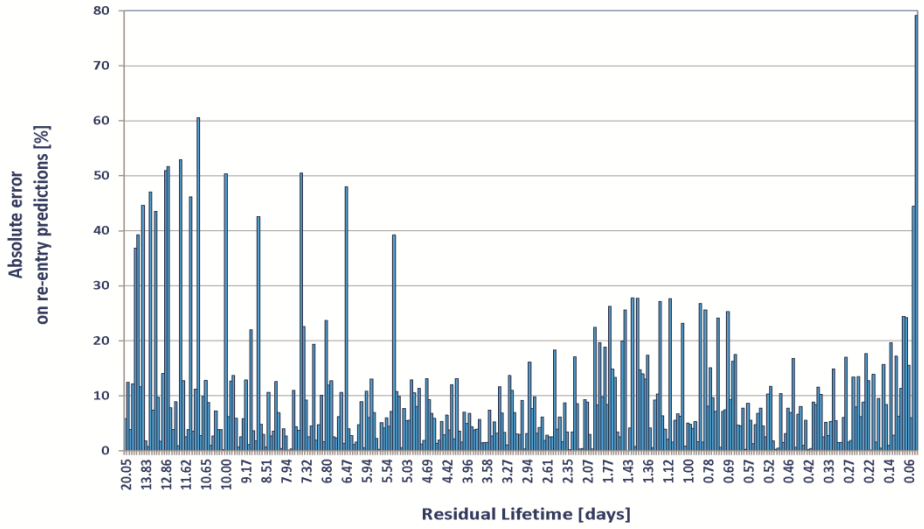


Figure 9. Percentage absolute errors associated with each re-entry prediction issued during all the IADC test campaigns, as a function of the residual lifetime

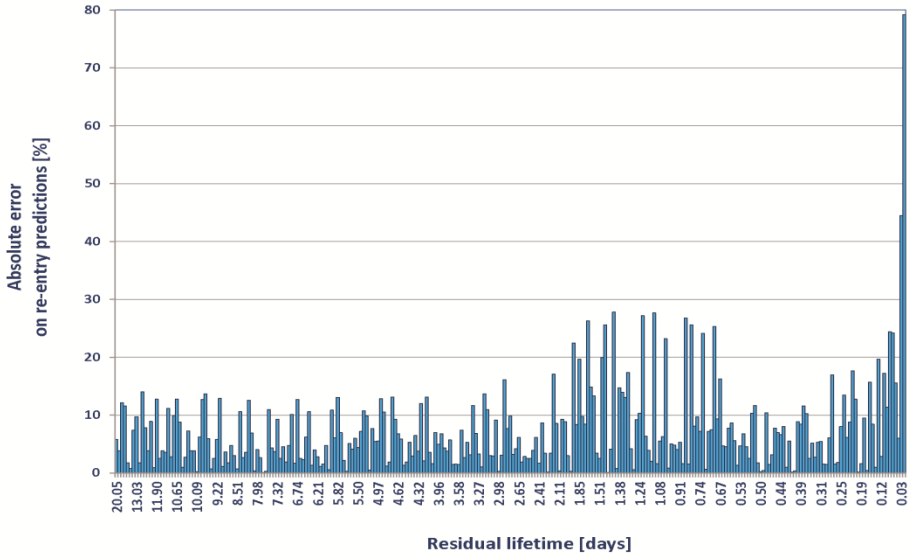


Figure 10. Percentage absolute errors associated with each re-entry prediction issued during the IADC test campaigns, excluding those involving GOCE and Molniya

Excluding again the GOCE and Molniya test campaigns, as well as the last "prediction" issued after the actual re-entry had occurred both for GFZ-1 and the Vostok upper stage re-entered in 2002, the relative prediction errors with absolute values > 15% obtained during the IADC test campaigns are listed in Tab. 3. It should be emphasized that all the cases occurred in the last 3 days before re-entry: 12% between 3 and 2 days, 36% between 2 and 1 day, and 52% during the last day. Moreover, 44% of the occurrences involved just one satellite of quite complicated shape, UARS, which presented a very complex behaviour during the final phase of its orbital decay, probably due to a sudden change of the attitude dynamics [24].

Another 24% of the occurrences involved, fifty-fifty, GFZ-1 and Coronas F, while the remaining 32% was shared by 5 other objects, 4 satellites and 1 upper stage.

Table 3. Relative re-entry prediction errors with absolute values > 15% obtained during the IADC test campaigns, excluding GOCE, Molniya and the last "prediction" for GFZ-1 and the Vostok upper stage re-entered in 2002.

| Satellite name | Residual lifetime [days] | Absolute value of the relative re-entry prediction error [%] |
|---|---|---|
| GFZ-1 | 1.425 | 27.78 |
| UARS | 1.097 | 27.66 |
| UARS | 1.219 | 27.16 |
| UARS | 0.853 | 26.77 |
| UARS | 1.709 | 26.25 |
| UARS | 1.465 | 25.61 |
| UARS | 0.792 | 25.59 |
| GFZ-1 | 0.694 | 25.30 |
| Cosmos 2332 | 0.088 | 24.41 |
| Cosmos 2332 | 0.066 | 24.21 |
| UARS | 0.731 | 24.12 |
| UARS | 1.036 | 23.19 |
| UARS | 2.016 | 22.46 |
| Coronas F | 1.492 | 19.93 |
| ROSAT | 0.127 | 19.67 |
| GFZ-1 | 1.851 | 19.65 |
| Vostok (2002) | 0.220 | 17.67 |
| Coronas F | 1.363 | 17.37 |
| EAS | 0.109 | 17.20 |
| Coronas F | 2.284 | 17.09 |
| Vostok (2002) | 0.270 | 16.97 |
| UARS | 0.670 | 16.27 |
| UARS | 2.753 | 16.12 |
| EAS | 0.155 | 15.69 |
| Cosmos 398 | 0.062 | 15.56 |

If only the IADC campaigns involving spent upper stages were taken into account, the prediction errors resulted to be relatively smaller, both in the maximum and average values. Fig. 11 shows the absolute values of the relative prediction errors obtained for the 86 re-entry predictions issued for upper stages. The average percentage error was 5.2% overall, 6.8% during the last two days, and 7.5% in the last day. If the largest prediction errors, associated with the Vostok upper stage re-entered at the maximum of solar cycle 23 in 2002, were taken away, still smaller prediction errors resulted for the upper stages, as shown in Fig. 12. In fact, the average percentage error, based on 74 re-entry predictions, decreased to 4.2% overall, to 4.1% in the last two days, and to 4.1% during the last day.

Among the 86 re-entry predictions for upper stages, only three had percentage errors > 15%, all associated with the Vostok upper stage re-entered in 2002 at the maximum of solar cycle 23 and issued less than six and half hours before re-entry.

Another relevant outcome of this statistical analysis is the distribution of the relative prediction errors. Tab. 4 shows the results obtained for the 316 re-entry predictions issued for all the objects. From these results it is quite clear that, in general, an absolute percentage error, in the residual lifetime, of 20% is needed to include nearly 90% of the cases, while an error of 30% would still fall slightly short of the 95% of the cases.

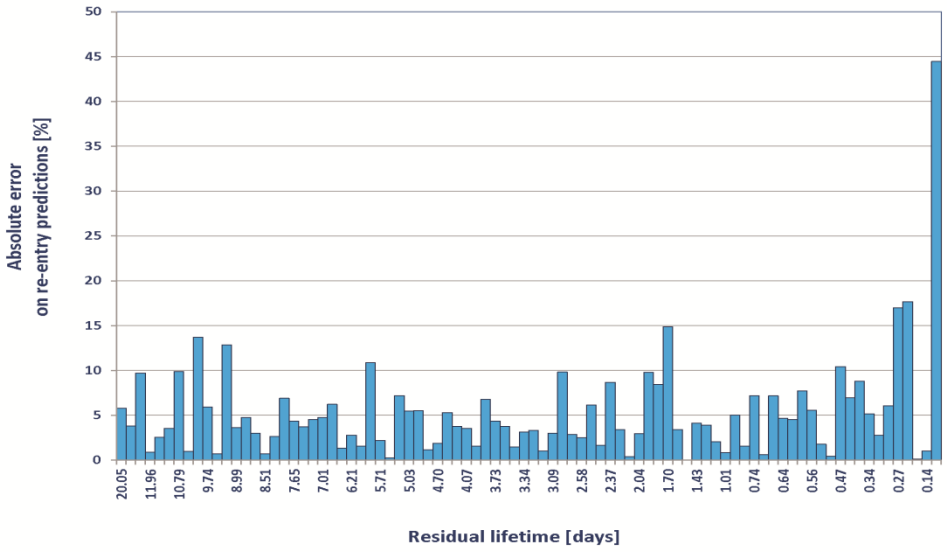


Figure 11. Percentage absolute errors associated with the IADC test campaigns for spent upper stages, as a function of the residual lifetime

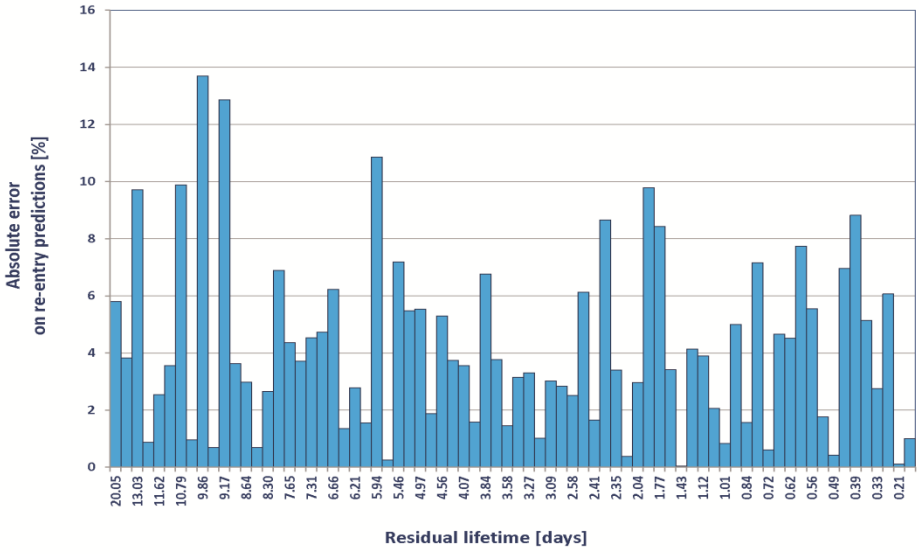


Figure 12. Percentage absolute errors associated with the IADC test campaigns for spent upper stages, excluding the Vostok stage re-entered in 2002

The situation during the last two days preceding the re-entry is illustrated in Tab. 5. Following these results, an absolute percentage error of 20% would not be able to include 90% of the cases, while an error

of 30% would embrace more than 98% of the occurrences (actually 100%, excluding the last prediction for GFZ-1 and the Vostok upper stage re-entered in 2002).

Table 4. Distribution of the absolute values of the relative errors for the re-entry predictions issued during the IADC test campaigns.

| Absolute percentage prediction error within | Number of re-entry predictions included | Percentage of re-entry predictions included |
|---|---|---|
| 80% | 316 | 100 |
| 70% | 315 | 99.7 |
| 60% | 314 | 99.4 |
| 50% | 309 | 97.8 |
| 45% | 306 | 96.8 |
| 40% | 302 | 95.6 |
| 35% | 299 | 94.6 |
| 30% | 299 | 94.6 |
| 25% | 290 | 91.8 |
| 20% | 282 | 89.2 |
| 15% | 264 | 83.5 |
| 10% | 218 | 69.0 |
| 5% | 133 | 42.1 |

Table 5. Distribution of the absolute values of the relative errors for the re-entry predictions issued during the last two days of the IADC test campaigns

| Absolute percentage prediction error within | Number of re-entry predictions included | Percentage of re-entry predictions included |
|---|---|---|
| 80% | 127 | 100 |
| 70% | 126 | 99.2 |
| 60% | 126 | 99.2 |
| 50% | 126 | 99.2 |
| 40% | 125 | 98.4 |
| 35% | 125 | 98.4 |
| 30% | 125 | 98.4 |
| 25% | 116 | 91.3 |
| 20% | 112 | 88.2 |
| 15% | 98 | 77.2 |
| 10% | 81 | 63.8 |
| 5% | 42 | 33.1 |

Tab. 6 reflects the situation for the 91 re-entry predictions issued during the last 24 hours before re-entry. This time, an absolute percentage error of 20% would be able to include more than 90% of the cases, while an error of 30% would still comprise nearly 98% of the occurrences.

Table 6. Distribution of the absolute values of the relative errors for the re-entry predictions issued during the last day of the IADC test campaigns.

| Absolute percentage prediction error within | Number of re-entry predictions included | Percentage of re-entry predictions included |
|---|---|---|
| 80% | 91 | 100 |
| 70% | 90 | 98.9 |
| 60% | 90 | 98.9 |
| 50% | 90 | 98.9 |
| 40% | 89 | 97.8 |
| 30% | 89 | 97.8 |
| 25% | 86 | 94.5 |
| 20% | 83 | 91.2 |
| 15% | 73 | 80.2 |
| 10% | 62 | 68.1 |
| 5% | 31 | 34.1 |

The results obtained, summarized in Tabs. 4-6, support the criteria adopted during the last three IADC campaigns (18-20) for the definition of re-entry uncertainty windows with an a priori confidence level of at least 90%. In fact, as previously recalled, a percentage error of ±20% on the residual lifetime was adopted up to 12 days before re-entry, then the uncertainty window was linearly increased, during the following 10 days, up to a variation of ±30%, applied during the last two days.

Table 7. Distribution of the absolute values of the relative errors for the re-entry predictions issued during the IADC test campaigns, during the last two days and during the last day, excluding the propagations with initial state vector epochs lying in the last 6 hours before re-entry.

| Absolute percentage prediction error within | All re-entry predictions included [%] | Re-entry predictions during the last 2 days [%] | Re-entry predictions during the last day [%] |
|---|---|---|---|
| 70% | 100 | 100 | 100 |
| 60% | 99.6 | 100 | 100 |
| 50% | 97.9 | 100 | 100 |
| 40% | 95.5 | 100 | 100 |
| 30% | 94.9 | 100 | 100 |
| 25% | 91.8 | 91.3 | 95.6 |
| 20% | 89.7 | 89.4 | 94.1 |
| 15% | 85.3 | 77.9 | 86.8 |
| 10% | 70.5 | 68.3 | 76.5 |
| 5% | 43.8 | 37.5 | 41.2 |

Removing from the tally the 24 predictions with initial propagation epochs lying in the last six hours of residual lifetime, the results shown in Tab. 7 are obtained, with 292 predictions overall, 103 in the last two days and 67 during the last day. It is clear that neglecting the few predictions very close to re-entry leads

to an overall improvement of the statistics, with an absolute percentage error of 20% nearly able to guarantee a confidence level of 90% irrespective of the residual lifetime. This confirms that the predictions carried out in the proximity of a re-entry are generally affected by a relative error higher than average, but, when available, they are anyway very useful, in order to reduce the absolute time amplitude of the uncertainty windows.

If, in addition to the 24 predictions with initial propagation epochs lying in the last six hours of residual lifetime, also all those issued for the Molniya and GOCE satellites are neglected, the results shown in Tab. 8 and Fig. 13 are obtained. However, no significant improvement was observed with respect to the results presented in Tab. 7 for an absolute percentage error of 20%, even though an error of 30% was able to cover all the occurrences, irrespective of the residual lifetime.

Table 8. Distribution of the absolute values of the relative errors for the re-entry predictions issued during the IADC test campaigns, during the last two days and during the last day, excluding, in addition to the propagations with initial state vector epochs lying in the last 6 hours before re-entry, all those for GOCE and Molniya.

| Absolute percentage prediction error within | All re-entry predictions included [%] | Re-entry predictions during the last 2 days [%] | Re-entry predictions during the last day [%] |
|---|---|---|---|
| 30% | 100 | 100 | 100 |
| 25% | 96.8 | 91.4 | 93.3 |
| 20% | 95.6 | 89.2 | 93.3 |
| 15% | 92.9 | 83.9 | 90.0 |
| 10% | 78.3 | 72.0 | 81.7 |
| 5% | 49.0 | 38.7 | 41.7 |

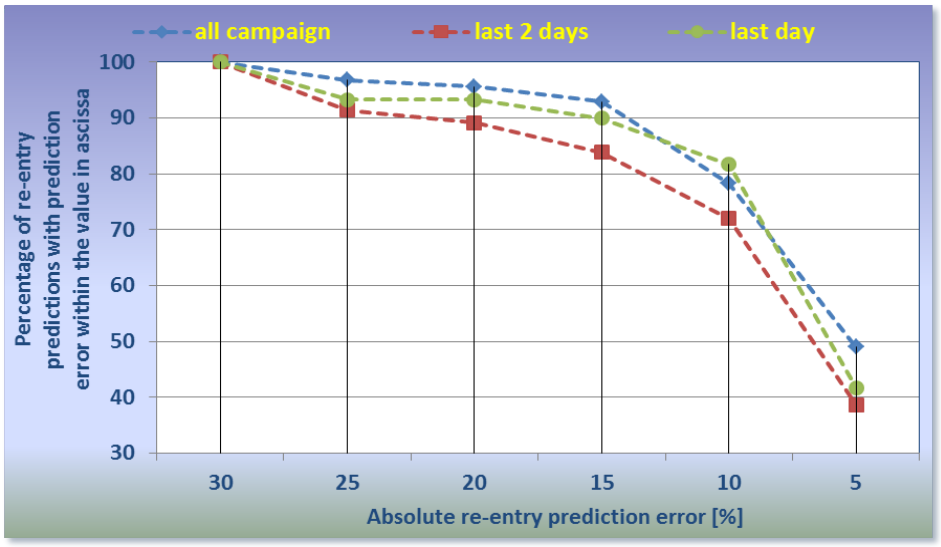


Figure 13. Distribution of the absolute values of the relative prediction errors, excluding the re-entry forecasts issued for GOCE and Molniya, as well as those with initial state vector epochs lying in the last six hours before re-entry

A mean prediction error, defined according to Eq. 4, was evaluated for each IADC re-entry campaign, as a function of the residual lifetime. For each campaign, this parameter shows the average absolute value of the prediction percentage error from any given time before re-entry to the re-entry reference epoch.

Plotting together all the results for each IADC test campaign, Fig. 14 was obtained. The average prediction errors encompassing the full duration of the 20 re-entry campaigns ranged from less than 5% to approximately 30%. Irrespective of the residual lifetime, the mean percentage errors remained below 20% in nearly 93% of the cases, but significantly higher mean errors were more probable during the last two days.

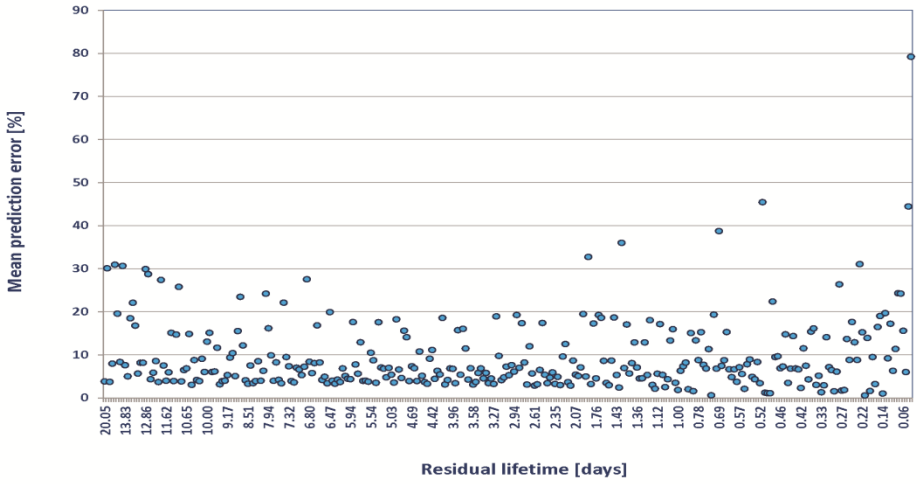


Figure 14. Mean prediction error versus residual lifetime for the 20 IADC test campaigns plotted together

Removing the GFZ-1, GOCE and Molniya campaigns from the plot (Fig. 15), the average prediction errors over the full duration of the campaigns ranged from less than 5% to 15%, while a mean percentage error greater than 20% occurred only in about 2% of the cases, all concentrated in the last 12 hours before re-entry.

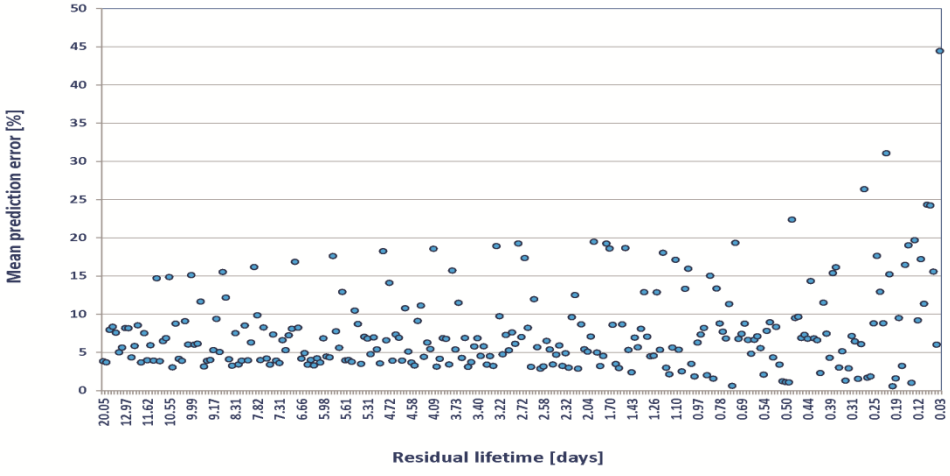


Figure 15. Mean prediction error versus residual lifetime for the IADC test campaigns excluding GFZ-1, GOCE and Molniya

In Fig. 16, only spacecraft and EAS were considered, while, in Fig. 17, GFZ-1, GOCE and Molniya were again neglected. Finally, the upper stages alone were sorted out in Fig. 18, while, in Fig. 19, the Vostok rocket body re-entered in 2002 was deleted.

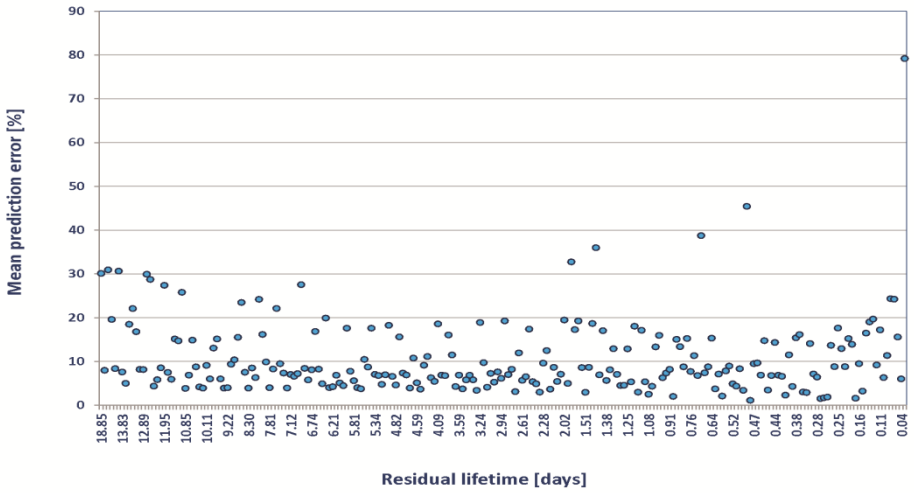


Figure 16. Mean prediction error for the IADC test campaigns including only spacecraft and EAS

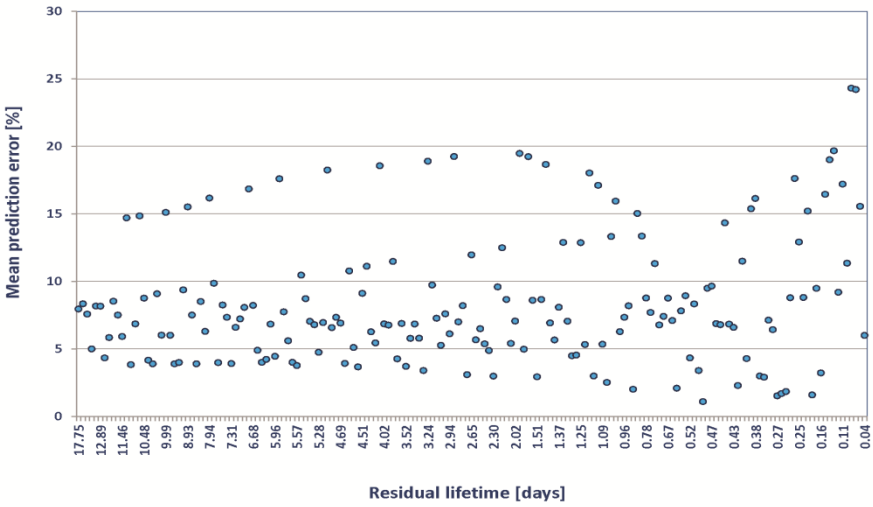


Figure 17. Mean prediction error for the IADC test campaigns including EAS and spacecraft, but ignoring GFZ-1, GOCE and Molniya

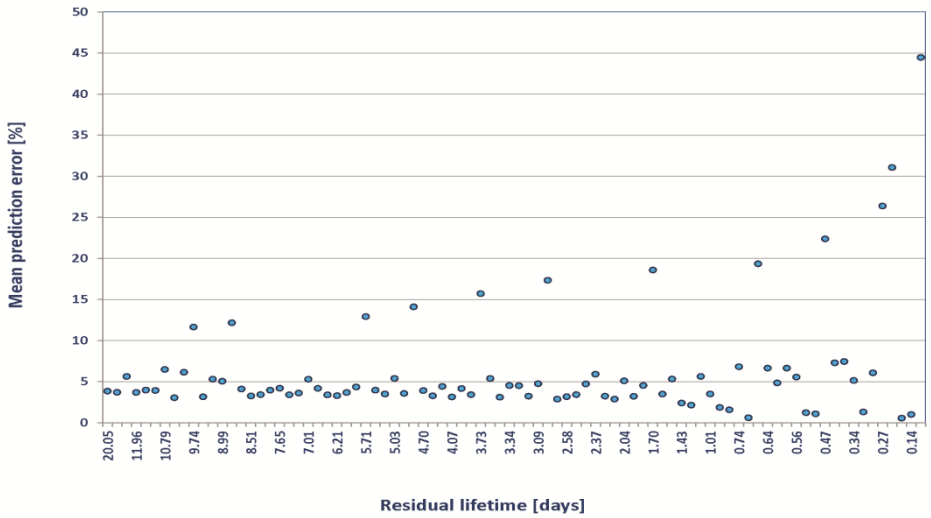


Figure 18. Mean prediction error for the IADC test campaigns including only upper stages

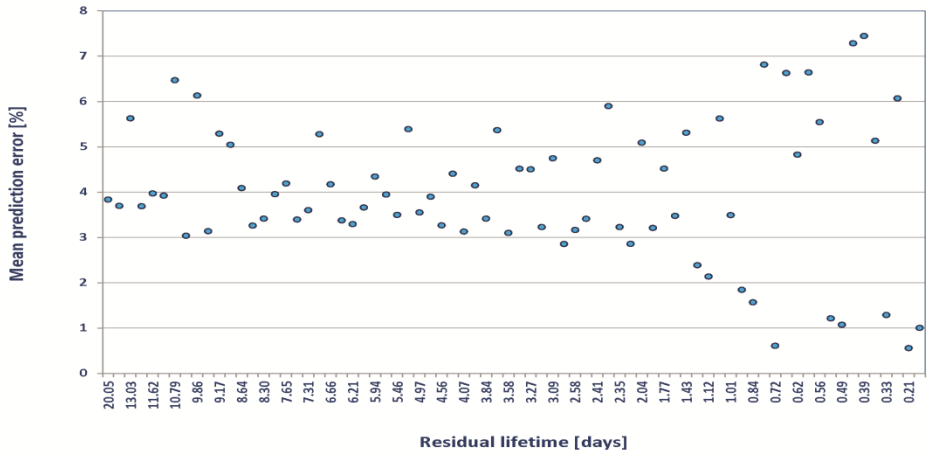


Figure 19. Mean prediction error for the IADC test campaigns including only upper stages, but ignoring the Vostok rocket body re-entered in 2002

Concerning the satellites (Figs. 16 and 17), the outcome was basically that already highlighted in Figs. 14 and 15. However, it should be remarked that, excluding from Fig. 17 also the UARS campaign, characterized by a quite complex decay behaviour and responsible of all the points between 15% and 20% up to 20 hours before re-entry, mean prediction errors lower than 15% were found in all the remaining spacecraft campaigns, up to 12 hours before re-entry.

Fig. 18 shows that results typically better than average were obtained for upper stages, with mean prediction errors around 5% over the complete campaigns and lower than 20% up to 18 hours before re-entry. This conclusion is even more evident if the campaign involving the Vostok stage re-entered in 2002 is excluded, as done in Fig. 19, leading to maximum mean prediction errors lower than 8% irrespective of the residual lifetime.

Eq. 4 was also applied not just separately to each campaign, as previously described, but also to all the 316 predictions issued for the 20 IADC test campaigns together. The results obtained are summarized in Fig. 20. Overall, as already pointed out, a mean prediction error of 9.7% was achieved. It was 8.5% during the last 10, 7 and 5 days, 9.3% during the last 3 days, 10.1% during the last 2 days, 9.8% during the last 36 hours, 9.4% during the last 24 hours, 9.8% during the last 12 hours, 15.0% during the last 6 hours, and 23.1% during the last 3 hours.

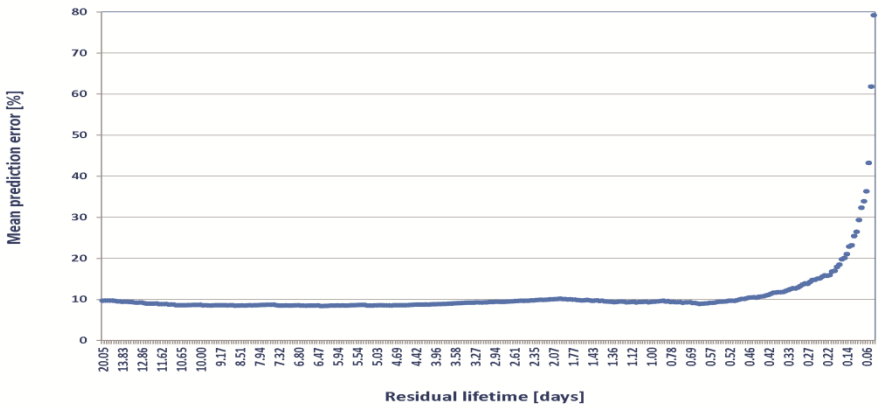


Figure 20. Mean prediction error versus residual lifetime considering together all the forecasts issued for the 20 IADC test campaigns

Excluding the GOCE and Molniya test campaigns, as well as the last prediction issued for GFZ-1 and the Vostok upper stage re-entered in 2002, the results summarized in Fig. 21 were obtained. Overall, a mean prediction error of 7.0% was achieved. It was 7.1% during the last 10 days, 7.4% during the last week, 7.7% during the last 5 days, 8.3% during the last 3 days, 8.9% during the last 2 days, 8.6% during the last 36 hours, 7.9% during the last 24 hours, 7.5% during the last 12 hours, 10.8% during the last 6 hours, and 14.5% during the last 3 hours.

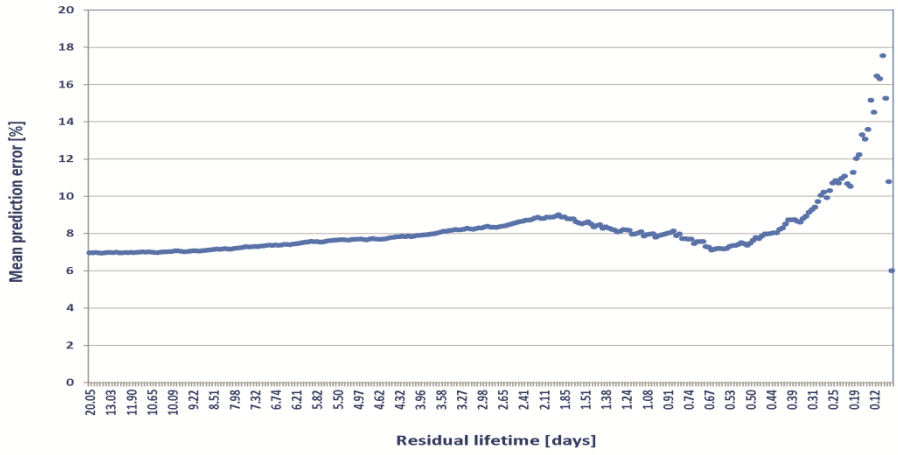


Figure 21. Mean prediction error considering all the forecasts issued to IADC, with the exception of GOCE, Molniya and the last predictions for GFZ-1 and the Vostok upper stage re-entered in 2002

## 7. Re-entries of potentially hazardous objects

Four out of twenty IADC exercises involved space objects considered potentially dangerous in some countries, Italy included, because their casualty expectancy was explicitly stated to exceed the alert threshold of $10^{-4}$. These objects were UARS, ROSAT, GOCE and Phobos-Grunt, for which ISTI-CNR was in charge also of the re-entry predictions for the Italian civil protection authorities, on behalf of the Italian Space Agency, in addition to the involvement in the IADC campaigns. Therefore, supplementary specific products were provided in these cases for civil protection applications [13,24,25]. Here, the attention is focused on a few aspects characterizing the re-entry of potentially hazardous space objects, as well as on the crucial information needed for risk mitigation purposes.

The criterion for the activation of a re-entry prediction campaign of national concern – in theory met whether an uncontrolled re-entering satellite, with a casualty expectancy alert threshold exceeding $10^{-4}$, overflies the Italian territory – was in effects satisfied for these IADC campaigns. As a matter of fact, the risk of human casualty associated with UARS was about 1:3200, in the latitude belt between ±57°, according to the re-entry survivability analysis performed by NASA, using the software tool ORSAT. The risk of human casualty from surviving debris from ROSAT was assessed by DLR (German Aerospace Centre), using SCARAB, to be around 1:3000, in the latitude belt between ±53°. For GOCE, the casualty expectancy was estimated to be slightly above the alert threshold, i.e. 1:5000, in the latitude belt between ±84°, but this re-entry presented a number of challenges, from the prediction and risk evaluation point of view, by reason of its peculiar nature [13]. For Phobos-Grunt, the risk of human casualty, in the latitude belt between ±52°, was assessed to be around 1:5000-1:3000, according to various estimates carried out in Russia and in Germany [24].

For these potentially hazardous re-entries, typical standard products, such as those provided during the IADC campaigns (i.e. the predicted nominal re-entry epoch with the associated uncertainty windows), are of very limited use for civil protection applications. In fact, the nominal decay forecast is absolutely useless for civil protection planning, due to its intrinsic large uncertainty. The associated uncertainty window provides, instead, significant information, designating the time interval inside which the re-entry should be expected somewhere in the world, within a given level of confidence. It is therefore clear that an appropriate and reliable definition of the re-entry uncertainty window associated with each nominal re-entry prediction is of paramount importance, being the most critical task when civil protection is involved in the process.

However, because the time span embraced by a sound uncertainty window remains very large until re-entry, causing the re-entry location to be left quite undetermined, no precautionary civil protection measure might be in practice devised and applied in advance. This means that locations possibly at risk in a given area, for instance in Italy, might not be alerted sufficiently ahead of re-entry with the simple knowledge of a "global" uncertainty window. For this reason, a new methodology was devised and applied in Italy to the campaigns involving the national civil protection authorities, since the re-entry of the BeppoSAX spacecraft, in 2003 [4,26].

In practice, having selected a specific (and relatively circumscribed) geographic area of interest, for instance Italy, for each possible re-entry opportunity included in the "global" uncertainty window and affecting the chosen area, a "regional" risk time window is estimated. The amplitude of each "regional" risk window is mainly a function of the different flight times of the fragments generated by the breakup of the re-entering object, and, in minor part, also depends on the variation of the initial conditions, as well as on the finite size of the area surrounding the simulated re-entry opportunity [25].

Considering the re-entry of typical spacecraft and upper stages, the amplitude of a "regional" risk time window embracing Italy is around 30-40 minutes long, including the airspace up to an altitude of 10-20

km, and even small particles not dangerous on the ground, but possibly representing a hazard for aircraft crossing the affected airspace. Finally, a cross-track safety margin, typically with amplitude of several tens of kilometres, is adopted around each simulated re-entry ground track, corresponding to each re-entry opportunity, in order to obtain the volume of airspace and the surface on the ground associated with every "regional" risk time window.

The procedure adopted at ISTI-CNR to assess the "regional" risk time windows for Italy typically starts 3-4 days before re-entry, giving sufficient time to the national civil protection authorities for familiarizing with the potential re-entry opportunities and planning possible risk mitigation measures. The "regional" risk time windows and the corresponding ground tracks with safety margins associated with each re-entry opportunity may be, in fact, estimated with a reasonable accuracy already a few days before the final decay, as a direct consequence of the almost perfect synchronization between the dynamical evolution of the re-entering object motion and of the Earth's rotation.

Of course, as the "global" uncertainty time window contracts approaching the final decay, some of the re-entry opportunities over the specific area of interest can be progressively excluded, focusing the attention on those still remaining a possibility. At the end, in most cases, all the re-entry opportunities over the area of interest can be definitely discarded before re-entry, as happened for UARS, ROSAT and GOCE respectively 5, 18 and 14 hours in advance (see e.g. Fig. 22, representing the ground track associated to the uncertainty window issued for GOCE at nearly 4 hours ahead re-entry). Sometimes, however, a re-entry over the area of interest cannot be excluded until the end, as happened with Phobos-Grunt for Italy (Fig. 23), and the related alert condition associated with the applicable "regional" risk window must be maintained until the closure of the window and, possibly, the re-entry confirmation.

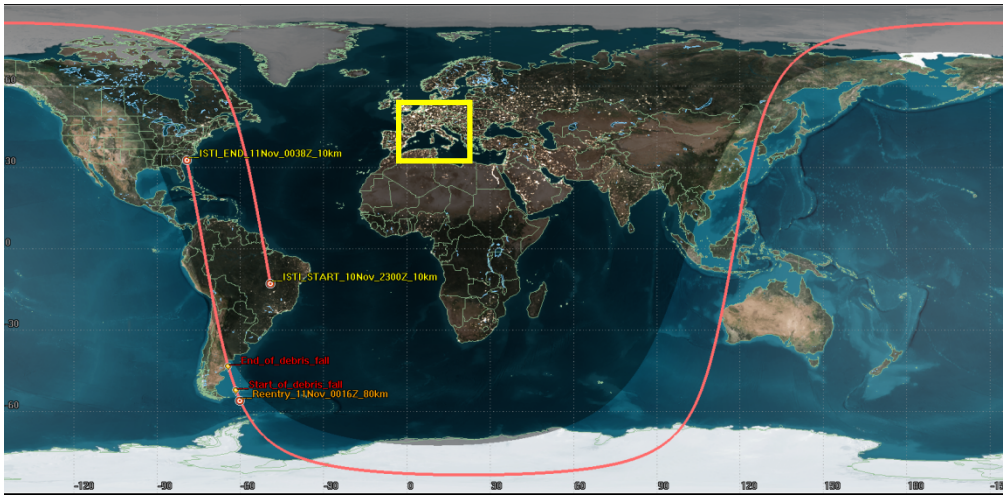


Figure 22. Ground track associated to the last uncertainty window issued by ISTI-CNR to IADC approximately 4 hours before re-entry. The GOCE fragments eventually plunged into the Southern Atlantic Ocean, between the Falkland Islands and the coast of Argentina, on 11 November 2013, between 00:24 and 00:40 UTC

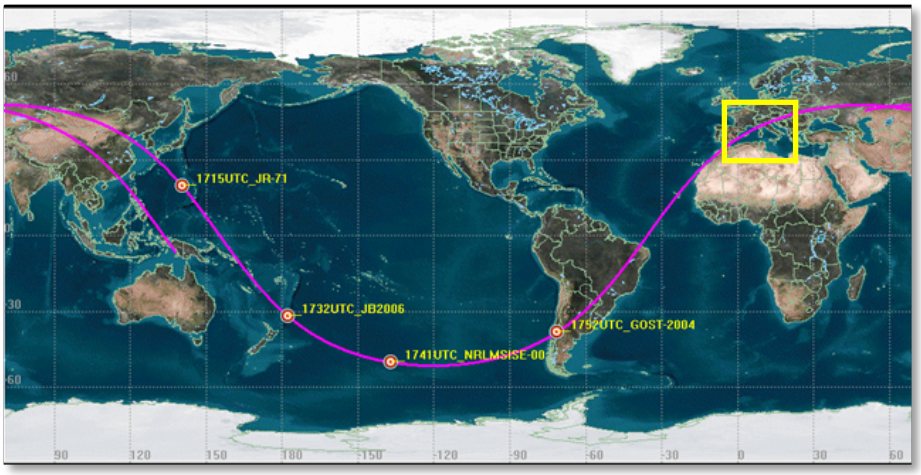


Figure 23. Ground-track associated to the last uncertainty window issued by ISTI-CNR to the Italian civil protection authorities approximately 1 hour before the Phobos-Grunt re-entry. The US Joint Space Operation Center (JSpOC) estimated that the re-entry at 80 km occurred at 17:46 UTC ± 1 min on 15 January 2012

## 8. Conclusions

The IADC re-entry test campaigns offered a very good opportunity to test and validate re-entry prediction approaches and tools. They also demonstrated that, thanks to the fully functional and efficient re-entry database hosted at ESA/ESOC, orbit data, re-entry predictions and supporting information can be easily and successfully shared among the worldwide participants during real re-entry exercises. Another relevant characteristic of these campaigns was having considered an appreciable variety of cases, covering both spacecraft and upper stages with quite different masses and shapes, as well as variable solar and geomagnetic activity conditions.

ISTI-CNR took part in all IADC campaigns, using its own software tools and methodologies, developed since 1979 to support the Italian civil protection needs. Among other things, different thermospheric density models were used and compared during the campaigns, generally showing a quite satisfactory agreement between them, and proving that most of the typical re-entry prediction errors are practically independent from the air density models used. On the other hand, the correlation between solar and geomagnetic activity conditions and the accuracy of re-entry predictions was not investigated in detail, mainly because the duration of the campaigns was short and only a relatively low number of them encompassed specific environmental conditions. A number of minor to strong geomagnetic storms were recorded during some campaigns, but none occurred at less than two days from re-entry.

The 316 re-entry predictions issued by ISTI-CNR during the first 20 IADC test campaigns represented a treasure trove of statistical information concerning the prediction errors affecting the estimate of the residual lifetime. Overall, the mean prediction error was about 10% until 12 hours before re-entry, increasing to 15% during the last 6 hours, and to 23% during the last 3 hours. The re-entry predictions for upper stages resulted more accurate than average, with a mean percentage error of about 5%, becoming nearly 7% in the last 2 days, and approximately 8% during the last day.

Based on the statistical distribution of the predictions, an uncertainty window able to guarantee a confidence level of 90% should assume an amplitude of about ±20% around the computed nominal re-entry time, when the residual lifetime is greater than 2 days, and of about ±25% during the last 2 days

before re-entry. An uncertainty window amplitude of ±30% would be, instead, needed to achieve a confidence level ≥ 95%.

It was also found that the residual lifetimes were overestimated in approximately 40% of the cases, and underestimated in the remaining 60%, supporting the adoption of asymmetric re-entry uncertainty windows, with "tails" longer than "heads", as those resulting by varying of a given percentage the ballistic parameter with respect to the nominal value obtained for the re-entering object.

## 9. Acknowledgements

Part of the work was carried out in the framework of the ASI-INAF agreement No. 2015-028-R.0 on "Space Debris: support to IADC activities and pre-operational validation for SST".

The authors are also indebted to the IADC Re-Entry Database, managed by and hosted at ESA/ESOC, and to the IADC participating agencies, for the data provided and exchanged during the re-entry test campaigns.

## 10. References

[1] Pardini, C. & Anselmo, L. (2016). Reentry Predictions of Potentially Dangerous Uncontrolled Satellites: Challenges and Civil Protection Applications. In *STARDUST 2016 – Extended Abstracts Book*, University of Strathclyde, UK, pp. 16-18.

[2] Klinkrad, H., Fritsche, B., Lips, T. & Koppenwallner, G. (2006). Re-entry Prediction and On-Ground Risk Estimation. In *Space Debris: Models and Risk Analysis* (Ed. H. Klinkrad), Chapter 9, Springer Praxis Publishing Ltd., Chichester, UK, pp. 241-288.

[3] NASA Orbital Debris Program Office (2013). Reentry of Cataloged Objects. *Orbital Debris Quarterly News* **17**(2), 5-6.

[4] Anselmo, L. & Pardini, C. (2005). Computational Methods for Reentry Trajectories and Risk Assessment. *Advances in Space Research* **35**, 1343-1352.

[5] Ailor, W., Hallman, W., Steckel, G. & Weaver, M. (2005). Analysis of Reentered Debris and Implications for Survivability Modeling. In *Proc. of the Fourth European Conference on Space Debris* (Ed. D. Danesy), ESA SP-587, ESA Publications Division, European Space Agency, Noordwijk, The Netherlands, pp. 539-544.

[6] Pardini, C. & Anselmo, L. (2013). Re-entry Predictions for Uncontrolled Satellites: Results and Challenges. In *Proc. 6th IAASS Conference 'Safety is Not an Option'* (Ed. L. Ouwehand), ESA SP-715 (CD-ROM), European Space Agency, Noordwijk, The Netherlands.

[7] Nicollier, C. & Gass, V. (Eds.) (2015). *Our Space Environment, Opportunities, Stakes and Dangers*, EPFL Press, Lausanne, Switzerland.

[8] NASA (2012). Process for Limiting Orbital Debris, NASA-STD-8719.14, Revision A with Change 1. NASA Technical Standard, National Aeronautics and Space Administration, Washington, DC, USA, p. 44.

[9] European Space Debris Safety and Mitigation Standard Working Group (2004). European Code of Conduct for Space Debris Mitigation, Issue 1.0. EDMSWG, p. 7.

[10] ESA Space Debris Mitigation Working Group (2015). ESA Space Debris Mitigation Compliance Verification Guidelines, Issue 1. European Space Agency, p. 28.

[11] Cole, J.K., Young, L.W. & Jordan-Culler, T. (1997). Hazards of Falling Debris to People, Aircraft, and Watercraft. Sandia Report, SAND97-0805-UC-706, Sandia National Laboratories, Albuquerque, NM, USA.

[12] Lips, T. & Fritsche, B. (2005). A Comparison of Commonly used Re-entry Analysis Tools, *Acta Astronautica* **57**, 312-323.

[13] Pardini, C. & Anselmo, L. (2015). GOCE Reentry Predictions for the Italian Civil Protection Authorities. In *Proc. of the 5th International GOCE User Workshop* (Ed. L. Ouwehand), ESA SP-728 (DVD), European Space Agency, Noordwijk, The Netherlands.

[14] Cappellari, J.O., Velez, C.E. & Fuchs, A.J. (Eds.) (1976). Mathematical Theory of the Goddard Trajectory Determination System. NASA/GSFC Report, GSFC X-582-76-77, Greenbelt, MD, USA, pp. 4-33–4-53.

[15] Hedin, A.E. (1987). MSIS-86 Thermospheric Model. *Journal of Geophysical Research* **92**, 4649-4662.

[16] Hedin, A.E. (1991). Extension of the MSIS Thermosphere Model into the Middle and Lower Atmosphere. *Journal of Geophysical Research* **96**, 1159-1172.

[17] Picone, J.M., Hedin, A.E., Drop, D.P. & Lean, J. (2002). NRLMSISE-00 Empirical Model: Comparisons to Data and Standard Models. In *Astrodynamics 2001*, Advances in the Astronautical Sciences Series, Vol. 109, Univelt Inc., San Diego, CA, USA, pp. 1385-1398.

[18] Volkov, I.I. (2004). Earth's Upper Atmosphere Density Model for Ballistic Support of the Flight of Artificial Earth Satellites. GOST R 25645.166-2004. Publishing House of the Standards, Moscow, Russia.

[19] Bowman, B.R., Tobiska, W.K., Marcos, F.A. & Vallares, C. (2008). The JB2006 Empirical Thermospheric Density Model. *Journal of Atmospheric and Solar Terrestrial Physics* **70**, 774-793.

[20] Pardini, C. & Anselmo, L. (1994). SATRAP: Satellite Reentry Analysis Program. Internal Report C94-17, CNUCE Institute, Consiglio Nazionale delle Ricerche, CNR, Pisa, Italy.

[21] Pardini, C., Moe, K. & Anselmo, L. (2012). Thermospheric Density Model Biases at the 23rd Sunspot Maximum. *Planetary and Space Science* **67**, 130-146.

[22] Bowman, B.R., Tobiska, W.K., Marcos, F.A., Huang, C.Y., Lin, C.S. & Burke, W.J. (2008). A New Empirical Thermospheric Density Model JB2008 Using New Solar and Geomagnetic Indices. AIAA/AAS Astrodynamics Specialist Conference, Honolulu, Hawaii, USA, Paper AIAA 2008-6438.

[23] Pardini, C. & Anselmo, L. (2016). The Uncontrolled Reentry of Progress-M 27M. *Journal of Space Safety Engineering* **3**(3), 117-126.

[24] Anselmo, L. & Pardini, C. (2013). Satellite Reentry Predictions for the Italian Civil Protection Authorities. *Acta Astronautica* **87**, 163-181.

[25] Pardini, C. & Anselmo, L. (2015). Satellite Re-entry Prediction Products for Civil Protection Applications. In *Proc. 7th IAASS Conference 'Space Safety is No Accident"* (Eds. T. Sgobba & I. Rongier), Springer International Publishing, Switzerland, pp. 453-462.

[26] Anselmo, L. (2003). Risk Analysis and Management of the BeppoSAX Reentry. ISTI Technical Report 2003-TR-23, Pisa, Italy.